

Multicast Beamforming Optimization in Cloud-based Heterogeneous Terrestrial and Satellite Networks

Hongming Zhang, *Member, IEEE*, Chunxiao Jiang, *Senior Member, IEEE*, Jingjing Wang, *Student Member, IEEE*, Li Wang, *Senior Member, IEEE*, Yong Ren, *Senior Member, IEEE*, and Lajos Hanzo, *Fellow, IEEE*

Abstract—A cloud-based terrestrial-satellite network (CTSN) is conceived for supporting ubiquitous high-speed multimedia services. In the CTSN, the satellite and terrestrial base stations are connected to a cloud-computing based centralized processor (CP), where joint user scheduling and multicast beamforming are performed based on realistic imperfect channel state information (CSI). Specifically, pilot-assisted channel estimation is assumed. Then, we propose a successive convex approximation (SCA) based algorithm for generating the beamforming vectors at the CP, where specific quality of service (QoS) constraints are considered. In the proposed algorithm, the beamforming vectors are obtained by iteratively solving a convex optimization problem subject to tight convex constraints. We demonstrate that feasible solutions can be obtained by our algorithm, even for the case when the system's dimension is large. Both analytical and numerical results are provided for characterizing the performance of the CTSN. Our results qualify the tradeoff between the cooperation-aided multiantenna gain and the pilot overhead imposed by training the beamformers. Furthermore, the achievable rate of the CTSN is shown to be substantially eroded by the accuracy of CSI.

Index Terms—Cloud-based terrestrial-satellite network, imperfect CSI, physical layer multicasting, transmit beamforming, QoS, successive convex approximation.

I. INTRODUCTION

Terrestrial-satellite networks (TSNs) have been recognized as a compelling technology for extending the coverage area of the existing wireless networks [1–7]. Indeed, the coexistence of terrestrial and satellite networks are of great potential in achieving 100% geographic coverage for the next generation of wireless networks, especially for those areas where no terrestrial base station (BS) infrastructure can be employed.

The TSNs have the advantage of providing ubiquitous data services with full frequency reuse to network users. However, the realization of such an ambitious network requires a lot of research efforts for tackling the existing technical issues. One of the challenges is to deal with the excessive in-band interference. In cellular networks, this type of interference can be effectively controlled by the multi-cell cooperative processing concept [8, 9], where the terrestrial BSs collaborate during their downlink transmission and/or uplink reception via backhaul links. Recently, the cooperative TSNs have attracted considerable research attentions [2, 10–17]. In a cooperative

TSN, a satellite and the terrestrial BSs jointly provide down-link services for ground users by sharing the same frequency band [17]. However, as shown in [18], the attainable system performance can be severely degraded by the in-band interference. In general, the in-band interference can be mitigated with the aid of cooperation between the satellites and terrestrial BSs [17]. Nevertheless, it is challenging to design efficient in-band interference mitigation for supporting high-rate multimedia services [10, 14, 17].

On the other hand, the exploitation of the unlicensed spectrum serves as an important technique to cope with the exponentially increasing teletraffic. Specifically, considerable research attention has been paid to the 30-90 GHz millimeter-wave (mmWave) frequency band for the next generation cellular networks [19], while the 26.5-40 GHz Ka band has been considered for supporting high speed satellite broadband services [5]. Thus, the satellite networks and the terrestrial cellular networks may coexist as well as share the same spectrum, say, in the 30-40 GHz band for example, in the next generation wireless networks [7, 20]. In particular, the performance of satellite communication systems operated in the Ka-band may be severely degraded by the atmospheric impairments, such as rain attenuation, increased noise temperature, depolarization, etc. Typically, these impairments can be classified into absorptive effects and non-absorptive effects [?]. The absorptive effects, such as gaseous absorption, cloud attenuation, rain attenuation, are typically quite substantial. By contrast, the non-absorptive effects, such as tropospheric scintillation, may result in rapid magnitude and phase fluctuation. Since the above-mentioned impairments have a significant impact on the attainable performance of satellite systems, substantial research efforts have to be invested in developing powerful mitigation techniques [4, 18, 21, 22]. For example, on-board beamforming aided satellite communication systems are capable of providing near-constant received power for users on the ground by shaping the beamforming pattern, even in the face of rain attenuation [?].

From another point of view, to meet the increasing demand for flawless multimedia services, a fundamental paradigm shift is taking place from the connection-centric transmission model to the content-centric model in mobile applications [23]. Generally, an inefficient content delivery solution may result in network congestion. A remedy to this issue is the so-called physical layer multicasting beamforming [24], where a common content is transmitted to a specific group of users with

L. Hanzo would like to acknowledge the financial support of the Engineering and Physical Sciences Research Council projects EP/N004558/1, EP/PO34284/1, COALESCE, of the Royal Society's Global Challenges Research Fund Grant as well as of the European Research Council's Advanced Fellow Grant QuantCom.

the aid of the channel state information signalled back from the receiver to the transmitter side (CSIT) by exploiting the broadcast nature of wireless communications. The multicast beamforming problem was initially studied in [24], where the core problem was proved to be NP-hard. Moreover, approximate solutions to the NP-hard multicast BF problem were also provided in [24] by invoking the classic semidefinite relaxation (SDR) in combination with a randomization approach. Then, the multicast beamforming design was conceived in [25] by giving cognizance to the quality of service (QoS) and optimizing the max-min signal-to-interference-plus-noise ratio (SINR). Later in [26], the multicast beamforming problems were studied under QoS and max-min SINR constraints in cooperative multi-cell networks. Recently, the authors of [27] proposed a cloud radio access network (C-RAN) based content-centric multicast BF strategy. Multicast beamforming aided satellite communications was also investigated in [28, 29]. Recently, a joint beamforming and power allocation scheme was proposed for non-orthogonal multiple access (NOMA) based TSNs, showing that an improved sum-rate performance can be achieved [22]. In general, the above-mentioned beamforming design problems can be formulated as quadratically constrained quadratic programs (QCQPs) [30]. This non-convex problem can be solved directly by invoking the alternating direction method of multipliers (ADMM) based technique or its modified version [31]. Alternatively, a popular method offering a provably near-optimal solution in polynomial time is constituted by the classic semidefinite programming (SDP) relaxation [24, 30]. However, as shown in [25, 26], the SDR combined with randomization may be unable to generate feasible solutions when the problem's dimension is large. In this case, an alternative approach, which is known as the successive convex approximation (SCA) [32], can be employed. In [33], the SCA was used for multi-group multicast beamforming design, while in [34], conic quadratic programming was invoked for beamforming design. As an improvement, a feasible point pursuit SCA (FPP-SCA) technique was proposed in [35], where slack variables are used to sustain feasibility. An efficient FPP-SCA based beamforming design was conceived for the large-scale antenna arrays in [36], while in [37] a joint beamforming and antenna selection design was proposed by applying the SCA.

Against the above background, our contributions are summarized as follows.

- *The Cloud-based TSN (CTSN) concept is conceived for managing the in-band interference imposed by multicast transmission. In the CTSN, the satellite and the terrestrial base stations (BSs) are connected to a cloud-computing based centralized processor (CP) via their respective wireless and/or wired backhaul links. Based on the channel state information (CSI), user scheduling and beamforming weight design are carried out at the CP.*
- *We propose a SCA-based beamforming design algorithm for the CTSN under having realistic imperfect CSI at the CP. We first formulate the beamforming design problems considered under our QoS constraints as QCQPs, which*

are shown to be non-convex. Then, the SCA methodology is invoked for solving our beamforming design problems. Near-optimal solutions are obtained for the proposed SCA-based beamforming algorithm by iteratively solving a convex optimization problem subject to a tight convex restriction of the constraint sets. In this way, our proposed algorithm is capable of generating feasible solutions after few iterations. Hence, it is very efficient, especially when the system's dimension is large.

The rest of the paper is organized as follows. In Section II, the system model is detailed. Section III introduces the multicast beamforming design proposed for the CTSN. The system performance is analyzed in Section IV and studied by simulations in Section V. Finally, we offer our conclusions in Section VI.

Notation: We use the following notation throughout this paper: \mathbb{R} is the real field and \mathbb{C} is the complex field. Matrices and vectors are denoted by upper- and lower-case boldface letters, respectively. $\mathcal{CN}(a, b)$ denotes the complex Gaussian distribution with a mean of a and a variance of b . $\mathbb{E}[\cdot]$ and $\text{diag}\{\cdot\}$ are the expectation operator and diagonalization operator, respectively. For a matrix \mathbf{A} , $(\mathbf{A})^T$ and $(\cdot)^H$ denote its transpose and conjugate transpose, respectively. The ℓ_p -norm of a vector \mathbf{x} is denoted as $\|\mathbf{x}\|_p$. The identity matrix of size N is denoted as \mathbf{I}_N . $|\mathcal{A}|$ is the cardinality of a set \mathcal{A} .

II. SYSTEM MODEL

We consider the multimedia multicast CTSN scenario of Fig. 1, where the contents are delivered to ground users both by a multibeam satellite and by terrestrial BSs. Within the designated coverage area, we assume that cooperation is performed within each cluster, whilst the clusters do not cooperate. In this paper, we focus our attention on the case of a single cluster, where the interference emanating from other clusters is treated as noise. As shown in Fig. 1, each cluster is formed by N_S satellite antennas and M terrestrial BSs with N_B antennas each, where the same frequency band are allocated. We assume that the N_S satellite antennas and the MN_B terrestrial BS antennas are coordinated by a cloud-computing based CP. In order to facilitate multicast transmission in our CTSN, CSI is required at the AP. Below, let us detail the channel models used in this paper.

A. Channel Model

Let us assume a slowly varying channel model, where the channel envelop remains time-invariant during a multicast period containing L symbols. Both small-scale fading and large-scale fading are considered for modelling both the satellite and terrestrial BS channels. Explicitly, the channel vector spanning from the satellite to a single-antenna ground user u can be expressed as

$$\check{\mathbf{g}}_u = \sqrt{a_u} \mathbf{g}_u, \quad (1)$$

where $a_u \in \mathbb{R}$ is the distance-dependent path loss between the satellite and the single-antenna ground user u . Here, we assume that the channel's power gain between each antenna of the satellite and a given ground user is the same. In (1),

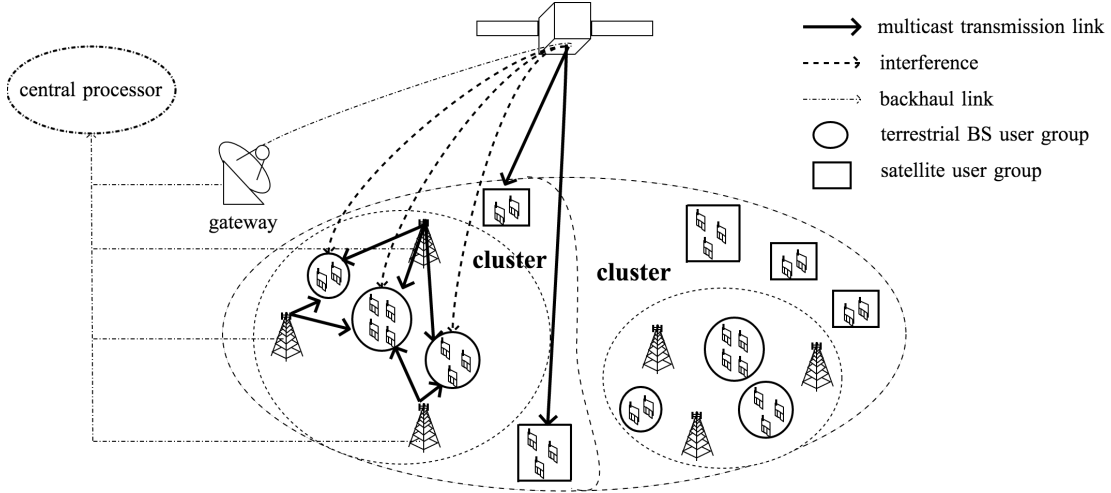


Fig. 1: Illustration of a multimedia multicast scenario in a cloud-based terrestrial-satellite network (CTSN), where the same frequency band is shared by users within a given cluster.

the small-scale term $\mathbf{g}_u = [g_u(0), \dots, g_u(N_S - 1)]^T \in \mathbb{C}^{N_S}$ contains the fading coefficients. Specifically, each fading coefficient $g_u(i)$ is assumed to obey the normalized shadowed-Rician model [38] associated with $g_u(i) = \Psi_i \exp\{j\chi_i\} + \Xi_i \exp\{j\zeta\}$, where χ_i is a uniform distributed phase over $[0, 2\pi)$ and ζ is a deterministic phase of the LOS component. Here, Ψ_i is an i.i.d. Rayleigh distributed random variable characterized by ϑ_1 being the average power of the scattered component. Furthermore, Ξ_i is an i.i.d. Nakagami distributed random variable characterized by (ϑ_2, Ω) , where ϑ_2 is the average power of the LOS component and Ω denotes the Nakagami parameter.

Similarly, the channel vector characterizing the link spanning from the terrestrial BS m to the single-antenna ground user u can be expressed as

$$\check{\mathbf{h}}_{m,u} = \sqrt{\alpha_{m,u}} \mathbf{h}_{m,u}, \quad (2)$$

where we have $\mathbf{h}_{m,u} = [h_{m,u}(0), \dots, h_{m,u}(N_B - 1)]^T \in \mathbb{C}^{N_B}$ with $h_{m,u}(i) \sim \mathcal{CN}(0, 1)$, $\forall i$. Moreover, the channel's power gain $\alpha_{m,u} \in \mathbb{R}$ between each antenna of the terrestrial BS m and a given ground user is also assumed to be the same.

B. CSI Acquisition and User Scheduling

We consider a frequency-division duplexing (FDD) system for obtaining the CSI at the CP. First, the terrestrial BSs and the satellite periodically broadcast messages to ground users in order to establish communication links with their prospective users. Generally, users within the coverage area of the terrestrial BSs receive messages from both the satellite and the terrestrial BSs, since the terrestrial BSs shown in Fig. 1 are within the coverage area of the satellite. In this case, communication links are established between these users and the terrestrial BSs, whilst any of the signals impinging from the satellite are treated as interference by these users. Specifically, we define these users as the terrestrial BS users in the following discussions. By contrast, the terrestrial BSs' message cannot be received by satellite users that are out of all

the BSs' coverage area due to the high propagation loss (i.e., $a_u \approx 0$ for the satellite user u). Hence, the satellite users can only establish communication links with the satellite, whilst they do not suffer interference from the terrestrial BSs.

As discussed, the CSI is required at the CP for its multicast transmission. In this paper, we assume that the pilot-assisted channel estimation scheme of [39] is employed for obtaining CSI. Let ηL symbols be reserved for pilot signaling during each L -symbol coherence interval, where $0 < \eta \leq 1$ is the fraction of pilot symbols. Recall that the terrestrial BS users suffer from interference imposed by the satellite's transmissions. Thus, the estimation of both the communication links and interfering links is required for the terrestrial BS users. By contrast, naturally, only the satellite links have to be estimated for the satellite users. In practice, only imperfect outdated and quantized CSI is obtained at the CP, as it will be detailed in Section III-A.

Next, the content download requests and the estimated downlink CSI of these users are sent to the CP via wired/wireless backhaul links. Here, the backhaul link capacity is assumed to be finite, hence, both the terrestrial BSs and the satellite are linked to the CP via finite capacity links. Furthermore, let us assume that a total of U_{tot} single-antenna users is scheduled to be served in a given frequency band during a pre-defined transmission period. Then, the U_{tot} users are partitioned into different multicast groups by the CP, where we consider a pragmatic user grouping strategy, which consists of two steps. Firstly, the U_{tot} users are first divided into U_S satellite users and U_B terrestrial BS users, where we have $U_{\text{tot}} = U_S + U_B$. Explicitly, the U_B terrestrial BS users and the U_S satellite users are served by the terrestrial BSs and the satellite, respectively. In the second step, the nearby users requesting the same content are grouped together at the CP. Note here that the content requests are only known at the CP, while the content information is assumed to be not shared by ground users. Let the U_{tot} users be grouped into $G_{\text{tot}} = G_S + G_B$ groups, including G_S satellite groups and

G_B terrestrial BS groups. Here, we have $1 \leq G_S \leq N_S$ and $1 \leq G_B \leq MN_B$. Note that this step can be implemented with the aid of the received requests and CSI of the ground users. Next, based on the received CSI, the transmit beamforming vectors of the G_{tot} multicast groups are designed by the CP. Before detailing the beamforming design, the signal model of the satellite and of the terrestrial BSs are detailed.

C. Signal Model

Let us first consider the satellite system. The index set of the i th satellite user group is denoted as $\mathcal{U}_{S,i}$, where we have $\sum_{i=1}^{G_S} |\mathcal{U}_{S,i}| = U_S$ and $\mathcal{U}_{S,i} \cap \mathcal{U}_{S,i'} = \emptyset$ for any $i \neq i'$. Furthermore, let us define the baseband equivalent multicast symbol of the i th satellite group as $s_i \in \mathbb{C}$, where we assume that s_i is independently drawn from a Gaussian codebook associated with $s_i \sim \mathcal{CN}(0, 1)$. Let us assume that a beamforming vector denoted as $\mathbf{w}_i \in \mathbb{C}^{N_S}$ is designed by the CP for multicast transmission to the i th group. Based on the above-mentioned user grouping strategy, the channels of satellite users belonging to the same group are assumed to be identical. Let $\check{\mathbf{g}}_i = \sqrt{a_i} \mathbf{g}_i$ denote the channel vector from the satellite to the i th group of users, where we have $\check{\mathbf{g}}_i = \check{\mathbf{g}}_{u_i}$ for any $u_i \in \mathcal{U}_{S,i}$. Note that in this case, the intra-group interference can be neglected. Hence, the received symbol of the satellite user $u_i \in \mathcal{U}_{S,i}$ can be expressed as

$$y_{u_i} = \underbrace{\check{\mathbf{g}}_i^H \mathbf{w}_i s_i}_{\text{desired signal}} + \underbrace{\sum_{i'=1, i' \neq i}^{G_S} \check{\mathbf{g}}_{i'}^H \mathbf{w}_{i'} s_{i'}}_{\text{interference}} + \underbrace{n_{u_i}}_{\text{noise}}, \quad (3)$$

where n_{u_i} denotes the complex additive white Gaussian noise with a mean of zero and a variance of one, i.e. we have $n_{u_i} \sim \mathcal{CN}(0, 1)$. Eq. (3) shows that each satellite user suffers from a certain level of inter-group interference, since the same frequency band is used by all the satellite user groups who are hence only separated on the basis of their different beam angles. Recall that the satellite users are not in the coverage areas of the terrestrial BSs, hence the interference imposed by the multicast transmission of the terrestrial BSs can be neglected for the satellite users. According to (3), the SINR of each satellite user $u_i \in \mathcal{U}_{S,i}$ can be formulated as

$$\gamma_{u_i} = \frac{|\check{\mathbf{g}}_i^H \mathbf{w}_i|^2}{\sum_{i'=1, i' \neq i}^{G_S} |\check{\mathbf{g}}_{i'}^H \mathbf{w}_{i'}|^2 + 1}. \quad (4)$$

On the other hand, since the terrestrial BS users are also within the coverage area of the satellite, the interference caused by the multicast transmission of the satellite cannot be neglected for the terrestrial BS users. Let $\mathcal{U}_{B,j}$ be the index set of the j th group of the terrestrial BS users, where we have $\sum_{j=1}^{G_B} |\mathcal{U}_{B,j}| = U_B$ and $\mathcal{U}_{B,j} \cap \mathcal{U}_{B,j'} = \emptyset$ for any $j \neq j'$. Moreover, let \mathbf{v}_j and s_j be, respectively, the transmit beamforming vector and the baseband equivalent multicast symbol generated by the CP for the j th group of the terrestrial BS users, where s_j is assumed to be independently drawn from a Gaussian codebook obeying $s_j \sim \mathcal{CN}(0, 1)$. Similarly, the

channels spanning from the satellite to the terrestrial BS users within the same group are assumed to be identical, where we have $\check{\mathbf{g}}_{u_j} = \check{\mathbf{g}}_j \triangleq \sqrt{a_j} \mathbf{g}_j$ for any $u_j \in \mathcal{U}_{B,j}$. By contrast, the channels between the terrestrial BSs and the ground users of the same group are different. In particular, the channel vector of each user is assumed to be unique, i.e. we have $\check{\mathbf{h}}_{m,u_j} \neq \check{\mathbf{h}}_{m,u'_j}$ for any $u_j \neq u'_j$. In this case, the received symbol of the terrestrial user $u_j \in \mathcal{U}_{B,j}$ can be formulated as

$$y_{u_j} = \underbrace{\check{\mathbf{h}}_{u_j}^H \mathbf{v}_j s_j}_{\text{desired signal}} + \underbrace{\sum_{j'=1, j' \neq j}^{G_B} \check{\mathbf{h}}_{u_j}^H \mathbf{v}_{j'} s_{j'}}_{\text{interference}} + \sum_{i=1}^{G_S} \check{\mathbf{g}}_i^H \mathbf{w}_i s_i + \underbrace{n_{u_j}}_{\text{noise}}, \quad (5)$$

where we have $\check{\mathbf{h}}_{u_j} = [\check{\mathbf{h}}_{1,u_j}^T, \dots, \check{\mathbf{h}}_{M,u_j}^T]^T \in \mathbb{C}^{MN_B}$, and the noise n_{u_j} is assumed to obey $n_{u_j} \sim \mathcal{CN}(0, 1)$. Finally, the SINR at the terrestrial user $u_j \in \mathcal{U}_{B,j}$ can be formulated as

$$\gamma_{u_j} = \frac{|\check{\mathbf{h}}_{u_j}^H \mathbf{v}_j|^2}{\sum_{j'=1, j' \neq j}^{G_B} |\check{\mathbf{h}}_{u_j}^H \mathbf{v}_{j'}|^2 + \sum_{i=1}^{G_S} |\check{\mathbf{g}}_i^H \mathbf{w}_i|^2 + 1}. \quad (6)$$

Clearly, the multicast transmission of the satellite imposes a certain level of inter-group interference on the terrestrial BS users in our CTSN. Hence, in order to support efficient multimedia transmission in the proposed CTSN, the transmit beamforming vectors of the terrestrial BSs and the satellite should be carefully designed by the CP, as detailed in the next section.

III. SUCCESSIVE CONVEX APPROXIMATION BASED BEAMFORMING DESIGN

In this section, we commence by introducing the imperfect CSI model to be used at the CP, followed by the beamforming design at the CP. Finally, we propose our SCA-based beamforming design for the CTSN considered.

A. Modeling of CSI at the Centralized Processor

As shown in Section II, the CP acquires the knowledge of two types of channel vectors. Explicitly, the first type is associated with the channels spanning from the satellite to all the ground users, i.e. the channel vectors $\check{\mathbf{g}}_i$ and $\check{\mathbf{g}}_j$ for $i = 1, \dots, G_S$ and $j = 1, \dots, G_B$, respectively. The second type is that spanning from the terrestrial BSs to the terrestrial BS users, which is denoted as $\check{\mathbf{h}}_{u_j}$ for $j = 1, \dots, G_B$. Generally, the corresponding distance-dependent path-loss term collected in the triplet $\{a_i, a_j, \alpha_{m,u_j}\}$ is related to the so-called geometry profile, which can be assumed to be known at the CP as the *a priori* information concerning its served users. Hence, we can focus our attention on the case where the small-scale term collected as $\{\mathbf{g}_i, \mathbf{g}_j, \mathbf{h}_{u_j}\}$ is imperfectly known to the CP. Let us assume that some partial information denoted as $\{\hat{\mathbf{g}}_i, \hat{\mathbf{g}}_j, \hat{\mathbf{h}}_{u_j}\}$ of these channels is obtained at the CP. Moreover, each channel coefficient in $\{\hat{\mathbf{g}}_i, \hat{\mathbf{g}}_j, \hat{\mathbf{h}}_{u_j}\}$ represents

the error-infested counterpart of $\{\mathbf{g}_i, \mathbf{g}_j, \mathbf{h}_{u_j}\}$. Then, we have the relationships of

$$\mathbf{g}_k = \hat{\mathbf{g}}_k + \mathbf{e}_k, \quad k = i \text{ or } j, \quad (7a)$$

$$\mathbf{h}_{u_j} = \hat{\mathbf{h}}_{u_j} + \mathbf{e}_{u_j}, \quad (7b)$$

where $\{\mathbf{e}_k, \mathbf{e}_{u_j}\}$ denotes the corresponding error imposed by channel estimation and the channel-contaminated transmission of CSI. More explicitly, transmission errors may be imposed by the uplink transmissions from both the ground users to the gateway and from the terrestrial BSs. For the sake of simplicity, we assume that the error symbol vectors in $\{\mathbf{e}_k, \mathbf{e}_{u_j}\}$ obey a complex Gaussian distribution with zero mean and a unified variance of σ_e^2 , where we have $0 \leq \sigma_e^2 < 1$. In our scenario, σ_e^2 is assumed to be unknown at the CP. Since only the imperfect channel knowledge of $\{\hat{\mathbf{g}}_i, \hat{\mathbf{g}}_j, \hat{\mathbf{h}}_{u_j}\}$ is available at the CP, the beamforming vectors have been designed based on the SINRs of

$$\hat{\gamma}_{u_i}^{\text{CP}} \triangleq \frac{a_i \left| \hat{\mathbf{g}}_i^H \mathbf{w}_i \right|^2}{\sum_{i'=1, i' \neq i}^{G_S} a_{i'} \left| \hat{\mathbf{g}}_{i'}^H \mathbf{w}_{i'} \right|^2 + 1} \quad (8)$$

and

$$\hat{\gamma}_{u_j}^{\text{CP}} \triangleq \frac{\left| \Lambda_{u_j} \hat{\mathbf{h}}_{u_j}^H \mathbf{v}_j \right|^2}{\sum_{j'=1, j' \neq j}^{G_B} \left| \Lambda_{u_j} \hat{\mathbf{h}}_{u_j}^H \mathbf{v}_{j'} \right|^2 + \sum_{i=1}^{G_S} a_i \left| \hat{\mathbf{g}}_i^H \mathbf{w}_i \right|^2 + 1}, \quad (9)$$

where, by definition, we have $\Lambda_{u_j} = \text{diag}\{\sqrt{\alpha_{1,u_j}} \mathbf{1}_{N_B}, \dots, \sqrt{\alpha_{M,u_j}} \mathbf{1}_{N_B}\}$ with $\mathbf{1}_{N_B} = \text{diag}\{\mathbf{I}_{N_B}\}$. Note that for the case of perfect CSI, we have $\mathbf{e}_i = \mathbf{e}_j = \mathbf{e}_{u_j} = \mathbf{0}$, $\hat{\gamma}_{u_i}^{\text{CP}} = \gamma_{u_i}$, and $\hat{\gamma}_{u_j}^{\text{CP}} = \gamma_{u_j}$.

B. Problem Statement

In this treatise, we focus our attention on the QoS design by providing a guaranteed minimum received SINR for every user in the CTSN. In particular, the same SINR target denoted as γ_{\min} is assumed for all the ground users. For the sake of comparison, let us first assume that cooperation is only invoked between the terrestrial BSs. More explicitly, in this case, the satellite does not cooperate with the terrestrial BSs, i.e. the gateway shown in Fig. 1 is not connected with the CP. Nonetheless, the same frequency band is used for both the satellite and the terrestrial BSs. Then, the satellite's beamforming design problem can be formulated as

$$\begin{aligned} & \min_{\{\mathbf{w}_1, \dots, \mathbf{w}_{G_S}\}} \sum_{i=1}^{G_S} \|\mathbf{w}_i\|_2^2 \\ & \text{subject to (s.t.) } \hat{\gamma}_{u_i}^S \geq \gamma_{\min}, \quad \forall u_i, \end{aligned} \quad (10)$$

where we have

$$\hat{\gamma}_{u_i}^S \triangleq \frac{a_i \left| \hat{\mathbf{g}}_i^H \mathbf{w}_i \right|^2}{\sum_{i'=1, i' \neq i}^{G_S} a_{i'} \left| \hat{\mathbf{g}}_{i'}^H \mathbf{w}_{i'} \right|^2 + 1}. \quad (11)$$

Since the multicast information of the satellite is unknown at the terrestrial BSs, beamforming vectors are designed at the

CP for mitigating the interference imposed by multicasting of the terrestrial BSs. In this case, the beamforming design for the terrestrial BS users under the SINR constraint γ_{\min} can be expressed as

$$\begin{aligned} & \min_{\{\mathbf{v}_1, \dots, \mathbf{v}_{G_B}\}} \sum_{j=1}^{G_B} \|\mathbf{v}_j\|_2^2 \\ & \text{s.t. } \hat{\gamma}_{u_j}^B \geq \gamma_{\min}, \quad \forall u_j, \end{aligned} \quad (12)$$

where we have

$$\hat{\gamma}_{u_j}^B \triangleq \frac{\left| \Lambda_{u_j} \hat{\mathbf{h}}_{u_j}^H \mathbf{v}_j \right|^2}{\sum_{j'=1, j' \neq j}^{G_B} \left| \Lambda_{u_j} \hat{\mathbf{h}}_{u_j}^H \mathbf{v}_{j'} \right|^2 + 1}. \quad (13)$$

In comparison to (9), the interference term imposed by the multimedia transmission of the satellite is omitted in the constraint of (12), since it is unknown at the CP. Clearly, the beamforming design problems of (10) and (12) are cast as the problems of minimizing the transmit power subject to meeting the SINR constraint of γ_{\min} . As shown in [24, 25], the core problem of the above formulations is NP-hard in general, but fortunately, its approximate solution may be found with the aid of SDP relaxation. Recalling that the terrestrial BS users suffer from the interference imposed by the satellite's multicast transmission, the solution of (12) may lead to a much lower exact SINR value than the targeted SINR γ_{\min} . As a result, the achievable rate of the whole system may be significantly reduced, especially when the number of terrestrial BS users is high, as it will be shown in Section V. Hence, our proposed CTSN detailed in Section II is a compelling system concept capable of addressing this issue. Below, let us detail the cooperative multicast beamforming design at the CP for our CTSN.

Since the CP has realistic CSI information about the scheduled users, the beamforming vectors of the satellite can be designed so that the interference term $\sum_{i=1}^{G_S} a_i \left| \hat{\mathbf{g}}_i^H \mathbf{w}_i \right|^2$ shown in (9) can be mitigated. In contrast to (10), we are now interested in the beamforming design problem of

$$\begin{aligned} & \min_{\{\mathbf{w}_1, \dots, \mathbf{w}_{G_S}\}} \sum_{i=1}^{G_S} a_i \left| \hat{\mathbf{g}}_i^H \mathbf{w}_i \right|^2 \\ & \text{s.t. } \hat{\gamma}_{u_i}^{\text{CP}} \geq \gamma_{\min}, \quad \forall u_i \end{aligned} \quad (14)$$

for $j = 1, \dots, G_B$. We point out here that the role of the beamforming vectors denoted as $\{\hat{\mathbf{w}}_1, \dots, \hat{\mathbf{w}}_{G_S}\}$ is two fold. Firstly, they are used for the multicast transmission of the satellite. Secondly, they are used for calculating the interference term of

$$\rho_j \triangleq \sum_{i=1}^{G_S} a_i \left| \hat{\mathbf{g}}_i^H \hat{\mathbf{w}}_i \right|^2, \quad (15)$$

which is furnished for the beamforming design of the terrestrial BSs. As soon as the interference term of (15) is

determined, the beamforming vectors of the terrestrial BSs can be designed at the CP by solving the optimization problem of

$$\begin{aligned} & \min_{\{\mathbf{v}_1, \dots, \mathbf{v}_{G_B}\}} \sum_{j=1}^{G_B} \|\mathbf{v}_j\|_2^2 \\ \text{s.t. } & \hat{\gamma}_{u_j}^{\text{CP}} \geq \gamma_{\min}, \quad \forall u_j, \end{aligned} \quad (16)$$

where $\hat{\gamma}_{u_j}^{\text{CP}}$ is shown in (9). Note here that in comparison to (12), more accurate SINR expressions are used in designing the beamforming vectors of the terrestrial BSs. Hence, the exact received SINRs become more similar to the target value, yielding an improved system capacity, as it will be shown in Section V.

Again, it can be readily shown that the problems of (14) and (16) are NP-hard in general. As suggested in [24], they can be relaxed to standard SDR problems and can be solved by some interior point methods. However, the authors of [25, 34] have suggested that the SDR combined with randomization may result in infeasible solutions, when the system's dimension is high. In order to tackle this problem, we propose a SCA-based beamforming design, as detailed next.

C. SCA-based Beamforming Design

To make our notation more concise, let us define the following quadratic function

$$f_k(\mathbf{x}_i) \triangleq a_k \left| \hat{\mathbf{g}}_k^H \mathbf{x}_i \right|^2 = a_k \mathbf{x}_i^H \hat{\mathbf{R}}_k \mathbf{x}_i, \quad k = i \text{ or } j, \quad (17)$$

where the channel's correlation matrix is defined as $\hat{\mathbf{R}}_k \triangleq \hat{\mathbf{g}}_k \hat{\mathbf{g}}_k^H \in \mathbb{C}^{N_s \times N_s}$ for $k = i$ or j , which is a positive semidefinite Hermitian matrix. Hence, the quadratic function of (17) is convex for $k = i$ or j . Based on (17), let us rewrite (14) as

$$\begin{aligned} & \min_{\{\mathbf{w}_1, \dots, \mathbf{w}_{G_S}\}} \sum_{i=1}^{G_S} f_j(\mathbf{w}_i) \\ \text{s.t. } & \gamma_{\min} \sum_{i'=1, i' \neq i}^{G_S} f_i(\mathbf{w}_{i'}) + [-f_i(\mathbf{w}_i)] \\ & + \gamma_{\min} \leq 0, \quad i = 1, \dots, G_S, \end{aligned} \quad (18)$$

for $j = 1, \dots, G_B$. Here, the problem shown in (18) is non-convex, since the second term on the left-hand-side (LHS) of the constraint is concave. According to the definition of (17), we have $-f_i(\mathbf{x}_i) \leq 0$ for any \mathbf{x}_i . Then, it is not hard to show the validity of the following inequality

$$\begin{aligned} -f_i(\mathbf{w}_i - \mathbf{z}_i) &= -a_i (\mathbf{w}_i - \mathbf{z}_i)^H \hat{\mathbf{R}}_i (\mathbf{w}_i - \mathbf{z}_i) \\ &= -f_i(\mathbf{w}_i) + 2a_i \Re\{\mathbf{z}_i^H \hat{\mathbf{R}}_i \mathbf{w}_i\} \\ &\quad - f_i(\mathbf{z}_i) \\ &\leq 0, \quad i = 1, \dots, G_S, \end{aligned} \quad (19)$$

for any $\mathbf{z}_i \in \mathbb{C}^{N_s}$. Based on (19), we can readily show that for a given \mathbf{z}_i , the concave term is upper bounded by

$$-f_i(\mathbf{w}_i) \leq f_i(\mathbf{w}_i, \mathbf{z}_i), \quad (20)$$

where $f_i(\mathbf{w}_i, \mathbf{z}_i) \triangleq -2a_i \Re\{\mathbf{z}_i^H \hat{\mathbf{R}}_i \mathbf{w}_i\} + f_i(\mathbf{z}_i)$ implying a linear restriction on $[-f_i(\mathbf{w}_i)]$ with respect to \mathbf{w}_i around the

point \mathbf{z}_i . Here, the linear function $f_i(\mathbf{w}_i, \mathbf{z}_i)$ can be simplified to the approximate function of $[-f_i(\mathbf{w}_i)]$ for a given \mathbf{z}_i . Let us introduce an auxiliary variable ρ_S that serves as an upper bound on $\sum_{i=1}^{G_S} f_j(\mathbf{w}_i)$. Then, the optimization problem to be solved at the t th iteration can be formulated as

$$\begin{aligned} & \min_{\{\mathbf{w}_1, \dots, \mathbf{w}_{G_S}\}} \rho_S \\ \text{s.t. } & \sum_{i=1}^{G_S} f_j(\mathbf{w}_i) - \rho_S \leq 0 \\ & \gamma_{\min} \sum_{i'=1, i' \neq i}^{G_S} f_i(\mathbf{w}_{i'}) + f_i(\mathbf{w}_i, \mathbf{z}_i^{[t]}) \\ & + \gamma_{\min} \leq 0, \quad i = 1, \dots, G_S, \end{aligned} \quad (21)$$

where $\mathbf{z}_i^{[t]}$ denotes a feasible point at the t th iteration. In comparison to (18), the optimization problem of (21) is convex at each iteration, which can be solved in polynomial time. Let $\tilde{\mathbf{w}}_i^{[t]}$ denote the solution of (21) at the t th iteration. Then, an updating rule of $\mathbf{z}_i^{[t+1]} = \tilde{\mathbf{w}}_i^{[t]}$ is applied for the next iteration. Finally, the algorithm terminates, when a convergence point is reached.

Similarly, the optimization problem of (16) can be solved by adopting the same methodology. Due to the stringent space limit, the details are omitted. Upon introducing an auxiliary variable ρ_B , which serves as an upper bound on $\sum_{j=1}^{G_B} \|\mathbf{v}_j\|_2^2$, the optimization problem to be solved at the t th iteration can be formulated as

$$\begin{aligned} & \min_{\{\mathbf{v}_1, \dots, \mathbf{v}_{G_B}\}} \rho_B \\ \text{s.t. } & \sum_{j=1}^{G_B} f(\mathbf{v}_j) - \rho_B \leq 0 \\ & \gamma_{\min} \sum_{j'=1, j' \neq j}^{G_B} f_{u_j}(\mathbf{v}_{j'}) + f_{u_j}(\mathbf{v}_j, \mathbf{z}_j^{[t]}) \\ & + \gamma_{\min}(1 + \rho_j) \leq 0, \quad \forall u_j, \end{aligned} \quad (22)$$

where by definition, we have

$$f(\mathbf{v}_j) \triangleq \|\mathbf{v}_j\|_2^2, \quad (23a)$$

$$f_{u_j}(\mathbf{v}_j) \triangleq \left| \mathbf{\Lambda}_{u_j} \hat{\mathbf{h}}_{u_j}^H \mathbf{v}_j \right|^2, \quad (23b)$$

$$\begin{aligned} f_{u_j}(\mathbf{v}_j, \mathbf{z}_j^{[t]}) &\triangleq -2\Re\left\{ \left(\mathbf{z}_j^{[t]} \right)^H \mathbf{\Lambda}_{u_j} \hat{\mathbf{R}}_{u_j} \mathbf{\Lambda}_{u_j}^H \mathbf{v}_j \right\} \\ &+ f_{u_j}(\mathbf{z}_j), \end{aligned} \quad (23c)$$

with $\hat{\mathbf{R}}_{u_j} \triangleq \hat{\mathbf{h}}_{u_j} \hat{\mathbf{h}}_{u_j}^H$. Finally, our proposed beamforming design is summarized in Algorithm 1.

Note that the beamforming design proposed for the CP is based on imperfect CSI, hence the beamforming vectors obtained are sub-optimal solutions in terms of the QoS at the ground users. In order to obtain the optimal solutions for this case, information concerning channel errors is required at the CP. However, we leave this problem for our future research. Clearly, a certain performance loss is expected due to the imperfect CSI at the CP, as discussed in the next section.

Algorithm 1 SCA-based Beamforming Design at the CP

Require: CSI

 1: **Initialization:** Set the maximum number of iterations to t_{stop} , the target SINR to γ_{min} , as well as generate initial feasible points $\mathbf{z}_i^{[0]}$ and $\mathbf{z}_j^{[0]}$ for $i = 1, \dots, G_S$ and $j = 1, \dots, G_B$, respectively.

 2: **for** $t = 1$ to t_{stop} **do**

 3: **repeat**

 4: Obtain the locally optimum $\{\tilde{\mathbf{w}}_1^{[t]}, \dots, \tilde{\mathbf{w}}_{G_S}^{[t]}\}$ by solving the following optimization problem

$$\begin{aligned} & \min_{\{\mathbf{w}_1, \dots, \mathbf{w}_{G_S}\}} \quad \rho_S \\ & \text{s. t.} \quad \sum_{i=1}^{G_S} f_j(\mathbf{w}_i) - \rho_S \leq 0 \\ & \quad \gamma_{\text{min}} \sum_{i'=1, i' \neq i}^{G_S} f_i(\mathbf{w}_{i'}) + f_i(\mathbf{w}_i, \mathbf{z}_i^{[t]}) \\ & \quad + \gamma_{\text{min}} \leq 0, \quad i = 1, \dots, G_S, \end{aligned}$$

 5: Update the feasible point as $\mathbf{z}_i^{[t+1]} = \tilde{\mathbf{w}}_i^{[t]}$ for $i = 1, \dots, G_S$.

 6: **until** Convergence

 7: **end for**

 8: Obtain the beamforming vectors $\{\hat{\mathbf{w}}_1, \dots, \hat{\mathbf{w}}_{G_S}\}$ for the satellite and calculate the interference of

$$\rho_j \triangleq \sum_{i=1}^{G_S} f_j(\hat{\mathbf{w}}_i)$$

 for $j = 1, \dots, G_S$.

 9: **for** $t = 1$ to t_{stop} **do**

 10: **repeat**

 11: Obtain the locally optimum $\{\tilde{\mathbf{v}}_1^{[t]}, \dots, \tilde{\mathbf{v}}_{G_B}^{[t]}\}$ by solving the following optimization problem

$$\begin{aligned} & \min_{\{\mathbf{v}_1, \dots, \mathbf{v}_{G_B}\}} \quad \rho_B \\ & \text{s. t.} \quad \sum_{j=1}^{G_B} f(\mathbf{v}_j) - \rho_B \leq 0 \\ & \quad \gamma_{\text{min}} \sum_{j'=1, j' \neq j}^{G_B} f_{u_j}(\mathbf{v}_{j'}) + f_{u_j}(\mathbf{v}_j, \mathbf{z}_j^{[t]}) \\ & \quad + \gamma_{\text{min}}(1 + \rho_j) \leq 0, \quad \forall u_j, \end{aligned}$$

 12: Update the feasible point as $\mathbf{z}_j^{[t+1]} = \tilde{\mathbf{v}}_j^{[t]}$ for $j = 1, \dots, G_B$.

 13: **until** Convergence

 14: **end for**

 15: Obtain the beamforming vectors $\{\hat{\mathbf{v}}_1, \dots, \hat{\mathbf{v}}_{G_B}\}$ for the terrestrial BSs.

 16: **return** $\{\hat{\mathbf{w}}_1, \dots, \hat{\mathbf{w}}_{G_S}\}$ and $\{\hat{\mathbf{v}}_1, \dots, \hat{\mathbf{v}}_{G_B}\}$.

IV. PERFORMANCE ANALYSIS

In this section, the performance of the CTSN is analyzed. We first provide analytical results of the achievable rate for the CTSN. Then, the feasibility of the proposed SCA-based algorithm conceived for beamforming design at the CP shown in Algorithm 1 is demonstrated.

A. Achievable Rate of the CTSN

We assume that the ground users do not cooperate with each other for the detection of multimedia symbols. Furthermore, we assume that $\{a_i, \hat{\mathbf{g}}_i, \hat{\mathbf{w}}_i\}$ and $\{\alpha_{m,u_j}, \hat{\mathbf{h}}_{u_j}, \hat{\mathbf{v}}_j\}$ are known at the corresponding satellite users and the corresponding terrestrial BS users, respectively. Then, each user detects his/her multimedia symbols with the aid of the knowledge of $\{a_i, \hat{\mathbf{g}}_i, \hat{\mathbf{w}}_i\}$ or $\{\alpha_{m,u_j}, \hat{\mathbf{h}}_{u_j}, \hat{\mathbf{v}}_j\}$. In detail, upon substituting

(7a) into (3), the received symbol of the satellite user $u_i \in \mathcal{U}_{S,i}$ can be formulated as

$$\begin{aligned} y_{u_i} = & \sqrt{a_i} \hat{\mathbf{g}}_i^H \hat{\mathbf{w}}_i s_i + \sum_{i'=1, i' \neq i}^{G_S} \sqrt{a_i} \hat{\mathbf{g}}_i^H \hat{\mathbf{w}}_{i'} s_{i'} \\ & + \sum_{i=1}^{G_S} \sqrt{a_i} \mathbf{e}_i^H \hat{\mathbf{w}}_i s_i + n_{u_i}, \end{aligned} \quad (24)$$

where the term $\sum_{i=1}^{G_S} \sqrt{a_i} \mathbf{e}_i^H \hat{\mathbf{w}}_i s_i$ is the intra-cluster multi-user interference caused by the imperfect CSI. Hence, the effective SINR at the i th group upon multimedia symbol detection is given by

$$\gamma_{u_i}^{\text{eff}} = \frac{f_i(\hat{\mathbf{w}}_i)}{\sum_{i'=1, i' \neq i}^{G_S} f_i(\hat{\mathbf{w}}_{i'}) + \sum_{i=1}^{G_S} \xi_i(\hat{\mathbf{w}}_i) + 1}, \quad (25)$$

where, by definition, we have $\xi_i(\hat{\mathbf{w}}_i) \triangleq a_i |\mathbf{e}_i^H \hat{\mathbf{w}}_i|^2$. Similarly, upon substituting (7a) and (7b) into (5), the received symbol of the terrestrial BS user $u_j \in \mathcal{U}_{B,j}$ can be formulated as

$$\begin{aligned} y_{u_j} = & \mathbf{\Lambda}_{u_j} \hat{\mathbf{h}}_{u_j}^H \hat{\mathbf{v}}_j s_j + \sum_{j'=1, j' \neq j}^{G_B} \mathbf{\Lambda}_{u_j} \\ & \hat{\mathbf{h}}_{u_j}^H \hat{\mathbf{v}}_{j'} s_{j'} + \sum_{j=1}^{G_S} \sqrt{a_j} \hat{\mathbf{g}}_j^H \hat{\mathbf{w}}_i s_i + \sum_{j=1}^{G_B} \mathbf{\Lambda}_{u_j} \mathbf{e}_{u_j}^H \hat{\mathbf{v}}_j s_j \\ & + \sum_{i=1}^{G_S} \sqrt{a_j} \mathbf{e}_j^H \hat{\mathbf{w}}_i s_i + n_{u_j} \end{aligned} \quad (26)$$

with the effective SINR of

$$\gamma_{u_j}^{\text{eff}} = \frac{f_{u_j}(\hat{\mathbf{v}}_j)}{\sum_{j'=1, j' \neq j}^{G_B} f_{u_j}(\hat{\mathbf{v}}_{j'}) + \sum_{j=1}^{G_B} \xi_{u_j}(\hat{\mathbf{v}}_j) + \sum_{i=1}^{G_S} \xi_j(\hat{\mathbf{w}}_i) + \rho_j + 1}, \quad (27)$$

where we have $\xi_{u_j}(\hat{\mathbf{v}}_j) \triangleq |\mathbf{\Lambda}_{u_j} \mathbf{e}_{u_j}^H \hat{\mathbf{v}}_j|^2$, as well as ρ_j is defined in (15). Since the beamforming vectors of the satellite and the terrestrial BSs are obtained based on the SINRs of (8) and (9), respectively, the corresponding effective SINRs shown in (25) and (27) are lower than the targeted SINR. Hence, the system performance will be degraded under the imperfect CSI.

Since the pilot-assisted CSI estimation of [39] is employed by our system described in Section II, the achievable rate of the CTSN is directly reduced by the pilot overhead. As shown in Section II, a total of ηL pilots are used for each multicast transmission, where $0 < \eta < 1$. Generally, the maximum number of channels that can be estimated is restricted by L . Hence, the total number of users that are scheduled by the CP for each multicast transmission is also limited. In particular, the quality of channel estimation may also be reduced by the so-called pilot contamination [40]. Let ψ be the pilot reuse factor, where the same orthogonal pilot sequences are reused by every ψ terrestrial BSs. Then, we have

$$N_S U_{\text{tot}} + M N_B U_B \leq \left\lfloor \frac{\eta L}{\psi} \right\rfloor, \quad (28)$$

where $\psi \geq 3$ is suggested for sufficiently mitigating pilot contamination [41].

Finally, by considering the pilot overhead, the average bandwidth efficiency in bits-per-second-per-Hertz-per-user (bits/s/Hz/user) of the proposed CTSN can be formulated as

$$C_{\text{CTSN}} = \frac{(1-\eta)L}{L} \frac{1}{U_{\text{tot}}} \mathbb{E} \left[\sum_{i=1}^{G_S} \sum_{u_i \in \mathcal{U}_{S,i}} \max_{p(s_i)} I(y_{u_i}; s_i | a_i, \hat{\mathbf{g}}_i, \hat{\mathbf{w}}_i) + \sum_{j=1}^{G_B} \sum_{u_j \in \mathcal{U}_{B,j}} \max_{p(s_j)} I(y_{u_j}; s_j | \mathbf{A}_{u_j}, \hat{\mathbf{h}}_{u_j}, \hat{\mathbf{v}}_j) \right], \quad (29)$$

where $p(s_i)$ and $p(s_j)$ are the distribution function of the multicast symbols of the satellite and the terrestrial BSs, respectively. Since random Gaussian signalling waveforms are assumed, we arrive at

$$C_{\text{CTSN}} = \frac{1-\eta}{U_{\text{tot}}} \left\{ \sum_{i=1}^{G_S} \sum_{u_i \in \mathcal{U}_{S,i}} \mathbb{E} [\log_2 (1 + \gamma_{u_i}^{\text{eff}})] + \sum_{j=1}^{G_B} \sum_{u_j \in \mathcal{U}_{B,j}} \mathbb{E} [\log_2 (1 + \gamma_{u_j}^{\text{eff}})] \right\}, \quad (30)$$

where the effective SINRs of $\gamma_{u_i}^{\text{eff}}$ and $\gamma_{u_j}^{\text{eff}}$ are given in (25) and (27), respectively.

B. Feasibility Analysis of Algorithm 1

For convenience, let us define the LHS of the constraints (18) and (21) as

$$g(\mathbf{W}_S) \triangleq \gamma_{\min} \sum_{i'=1, i' \neq i}^{G_S} f_i(\mathbf{w}_{i'}) + [-f_i(\mathbf{w}_i)] + \gamma_{\min}, \quad (31a)$$

$$h(\mathbf{W}_S, \mathbf{z}^{[t]}) \triangleq \gamma_{\min} \sum_{i'=1, i' \neq i}^{G_S} f_i(\mathbf{w}_{i'}) + f_i(\mathbf{w}_i, \mathbf{z}_i^{[t]}) + \gamma_{\min}, \text{ for } i = 1, \dots, G_S \quad (31b)$$

where, by definition, we have $\mathbf{W}_S \triangleq [\mathbf{w}_1, \dots, \mathbf{w}_{G_S}]$ and $\mathbf{z}^{[t]} = [\mathbf{z}_1^{[t]}, \dots, \mathbf{z}_{G_S}^{[t]}]$. Note that as shown in Section III-C, $g(\mathbf{W}_S)$ and $h(\mathbf{W}_S, \mathbf{z}^{[t]})$ are non-convex and convex, respectively. Then, for a given locally optimal solution denoted as $\widetilde{\mathbf{W}}_S^{[t]} = [\widetilde{\mathbf{w}}_1^{[t]}, \dots, \widetilde{\mathbf{w}}_{G_S}^{[t]}]$ at the t th iteration, the last constraint of (21) is satisfied, i.e. we have

$$h(\widetilde{\mathbf{W}}_S^{[t]}, \mathbf{z}^{[t]}) \leq 0. \quad (32)$$

Furthermore, according to (20) and (32), it can be readily shown that

$$g(\widetilde{\mathbf{W}}_S^{[t]}) \leq h(\widetilde{\mathbf{W}}_S^{[t]}, \mathbf{z}^{[t]}) \leq 0. \quad (33)$$

Thus, we can show that the locally optimal solution $\widetilde{\mathbf{W}}_S^{[t]}$ at the t th iteration is a feasible solution of the original nonconvex

problem of (18), since the nonconvex constraint in (18) is met by (33). Next, as shown in Algorithm 1, upon substituting $\mathbf{z}_i^{[t+1]} = \widetilde{\mathbf{w}}_i^{[t]}$, the relationship of (33) is also satisfied at the $(t+1)$ st iteration. Similarly, the same result can be shown for the beamforming design of terrestrial BSs, the detail of which is omitted. Therefore, we can now show that the proposed Algorithm 1 always generates feasible solutions. We shall point out here that since the above derivation is independent of the problem's dimension, the feasibility results still hold, when the problem's dimension is large.

V. NUMERICAL RESULTS

In this section, simulation results are provided for investigating the system performance of the CTSN. Specifically, we focus our attention on a single-cluster scenario in our CTSN, where a full spectrum reuse in Ka band with a central frequency of 18.7 GHz is considered [5], i.e. the spectrum reuse factor is set to 1. The system parameters are given in Table I. The height of each BS is set to be 11.4168 m. Moreover, the distance between any two terrestrial BSs is set to be 500 m. On the other hand, the satellite is assumed to have altitude of 1000 km. Furthermore, the coverage radius of the satellite is set to be 40 km. The ground users are uniformly distributed within the coverage area of a cluster. The path-loss experienced by the terrestrial BS users follows the 3GPP urban model given by $[52.87 + 37.6 \log_{10}(d_B)]$ in dB, where d_B denotes the distance between the terrestrial BS and a terrestrial BS user in meters. By contrast, the path loss of the satellite users is modelled by the free space model of $[57.88 + 20 \log_{10}(d_S)]$ in dB, where d_S is the distance between the terrestrial BS and a satellite user in meters. Moreover, two commonly used shadowing scenarios for satellite channels, namely frequent heavy shadowing (FHS) and infrequent light shadowing (ILS) [38], are given in Table I. The power spectral density of background noise is set to be -174 dBm/Hz, which is used for normalization. Both the satellite channels and terrestrial BS channels are assumed to be time-invariant during the transmission of $L = 2 \times 10^4$ symbols. The pilot reuse factor is set to $\psi = 7$. We consider G_S satellite groups and G_B terrestrial BS groups, each of which contains 2 single-antenna users, i.e., we have $|\mathcal{U}_{S,1}| = \dots = |\mathcal{U}_{S,G_S}| = |\mathcal{U}_{B,1}| = \dots = |\mathcal{U}_{B,G_B}| = 2$.

The SE performance of the non-cooperative TSN and the CTSN systems is compared in Fig. 2, where perfect CSI is assumed at the CP. In this figure, multicast servers are provided for $G_S = 2, 3$, and 4 satellite groups and $G_B = 4$ terrestrial BS groups. Each terrestrial BS is equipped with $N_B = 4$ transmit antennas (TAs), while $N_S = 4$ TAs of the satellite are employed for multicast transmission. Note that since the SE is measured in bits/s/Hz/users, the SE of the CSTN is identical for $G_S = 2, 3$, and 4. Observe from Fig. 2 that the attainable SE of the proposed CTSN is much higher than that of the non-cooperative system. Furthermore, as the number of satellite groups increases, the attainable SE of the non-cooperative system becomes degraded. These observations confirm our analysis provided in Section III-A. Since the satellite does not cooperate with the terrestrial BSs,

TABLE I: CTSN System Parameters

Central Frequency	18.7 GHz
BS-to-BS Distance	500 m
BS Height	11.4168 m
Satellite Altitude	10^6 m
Satellite Coverage Radius	4×10^4 m
Path Loss of BSs	$52.87 + 37.6 \log_{10}(d_B)$ dB
Path Loss of the satellite	$57.88 + 20 \log_{10}(d_S)$ dB
Frequent heavy shadowing of Satellite	$\vartheta_1 = 0.063, \vartheta_2 = 0.739, \Omega = 8.97 \times 10^{-4}$
Infrequent light shadowing of Satellite	$\vartheta_1 = 0.158, \vartheta_2 = 19.4, \Omega = 1.29$
PSD of Background Noise	-174 dBm/Hz
Pilot Reuse Factor	7
Frame Length	2×10^4

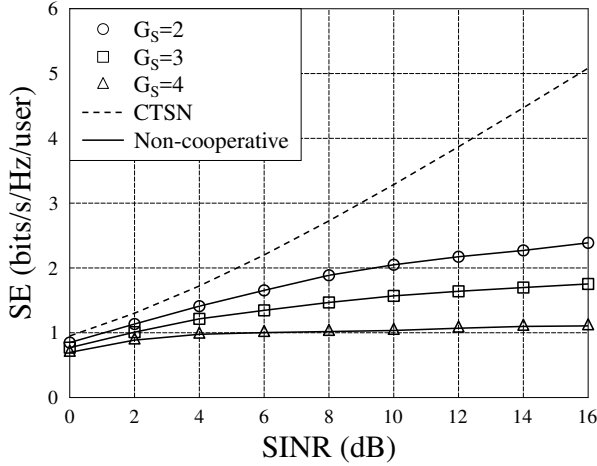


Fig. 2: Spectral efficiency (SE) versus the target SINR for both CTSN and non-cooperative TSN systems under perfect CSI, where Gaussian signalling waveforms are assumed. The satellite with $N_S = 4$ antennas supports G_S multicast groups. Two terrestrial BSs with $N_B = 4$ provide multicast services to $G_B = 4$ multicast groups.

the solution of (12) may result in a received SINR that is much lower than the targeted SINR. Hence, the corresponding SE may be significantly reduced. By contrast, the solution of (16) for the CTSN usually yields an SINR that is close to the targeted SINR. In this case, the attainable SE of the CTSN is higher than that of the non-cooperative system.

In Fig. 3, we investigate the convergence behaviors of our SCA-based Algorithm 1 conceived for our multicast beamforming aided CTSN, where perfect CSI is assumed at the CP. In this figure, the satellite equipped with $N_S = 4$ TAs serves $G_S = 4$ groups, whilst the terrestrial BSs with $N_B = 4$ support $G_B = 4$ groups. As shown in Fig. 3, Algorithm 1 converges within less than 6 iterations for both FHS and ILS scenarios. Furthermore, since our SCA-based algorithm is capable of taking advantage of the computationally efficient quadratic programming solver, it can be rendered as a fast algorithm for generating the beamforming weights at the CP.

Fig. 4 plots the average transmit power of the satellite and

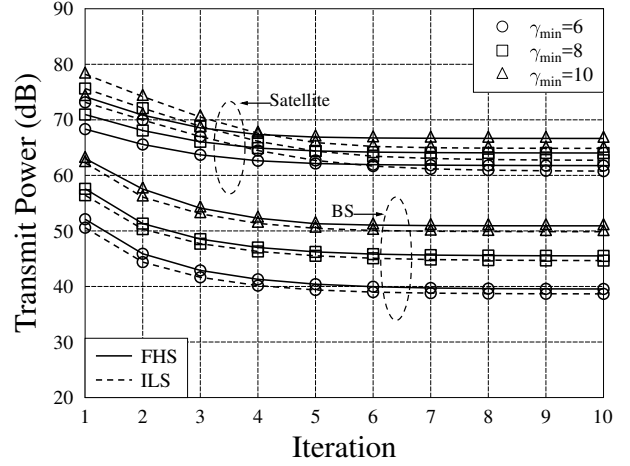


Fig. 3: Convergence behavior of the SCA-based algorithm invoked for the multicast beamforming design of the CTSN, where perfect CSI is assumed. The satellite using $N_S = 4$ TAs supports $G_S = 4$ multicast groups. Two terrestrial BSs using $N_B = 4$ provide multicast services to $G_B = 4$ multicast groups.

the terrestrial BSs in our CTSN under perfect CSI, when the proposed SCA-based beamforming design is used. In this figure, the satellite using $N_S = 4$ TAs provides multimedia service to $G_S = 2$ and 4 groups. Moreover, two terrestrial BSs with $N_B = 4$ support multicast services to $G_B = 4$ multicast groups. Based on the results of Fig. 4, we have the following observations. Firstly, the average transmit power consumed by the satellite is higher than that consumed by the terrestrial BSs. This is because the terrestrial BS users have a 20 dB/decade pathloss exponent and only a distance of 500 m, while the satellite users have 37.6 dB/decade and a distance of 1000 km. Thus, a higher transmit power is required by the satellite in order to attain the same target SINR. Secondly, as the number of satellite groups increases, the average transmit power consumed by the satellite and the terrestrial BSs increases. This observation can be explained as follows. Firstly, a higher transmit power is required by the satellite to support more multicast groups. Meanwhile, the terrestrial BS

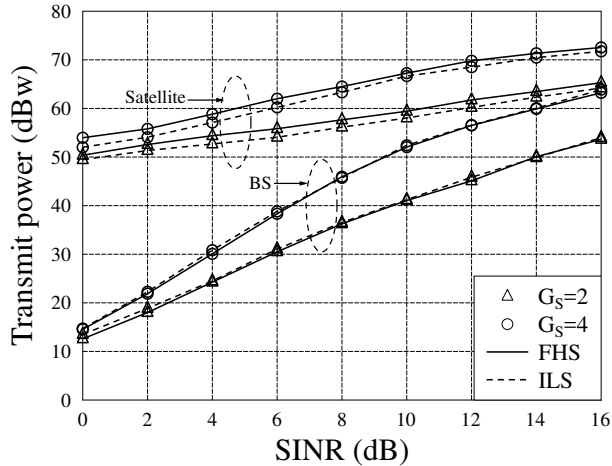


Fig. 4: Transmit power versus the target SINR for CTSN systems under perfect CSI, where Gaussian signalling waveforms are assumed. The satellite using $N_S = 4$ TAs supports G_S multicast groups. Two terrestrial BSs employing $N_B = 4$ provide multicast services to $G_B = 4$ multicast groups.

users suffer from higher interference imposed by the satellite multicasting. Hence, a higher transmit power is required by the terrestrial BSs in order to achieve the target SINR. Finally, as seen in Fig. 4, a higher satellite transmit power is required for attaining the target SINR in FHS scenarios in comparison to that required in ILS scenarios. This is because it was shown in [38] that, the channel gain of the satellite observed in FHS scenarios is higher than that in ILS scenarios. Hence a higher transmit power is required for attaining the same target SINR level at users. By contrast, almost the same BS transmit power is required for attaining the target SINR in both FHS and in ILS scenarios. This observation confirms the efficiency of our satellite beamforming design shown in Algorithm 1, which can be explained as follows. According to our satellite beamforming design shown in (14), the BS-aided users only have to tolerate the minimized level of interference imposed by the satellite multicast services for both FHS and ILS scenarios. In this case, the same transmit power is required by the terrestrial BSs to achieve the target SINR.

The sum rate performance of a cluster in the CTSN under perfect CSI is investigated in Fig. 5. In this figure, the number of satellite groups and terrestrial BS groups are $G_S = N_S$ and $G_B = MN_B$, respectively. As shown in Fig. 5, when the number of terrestrial BSs increases, the sum rate of the cluster first increases, and then decreases. Clearly, there is an optimal value for the number of terrestrial BSs, so that the sum rate of the cluster can be maximized. We can also observe from Fig. 5 that the larger the number of TAs of each BS, the faster the sum rate degrades. This is due to the tradeoff between the multiantenna gain and the pilot overhead. As analyzed in Section IV, the larger the number of cooperative BSs, the higher pilot overhead required for obtaining CSI at the CP. Hence, the sum rate of the cluster is decreased, when the improvement of multiantenna gain is unable to compensate for

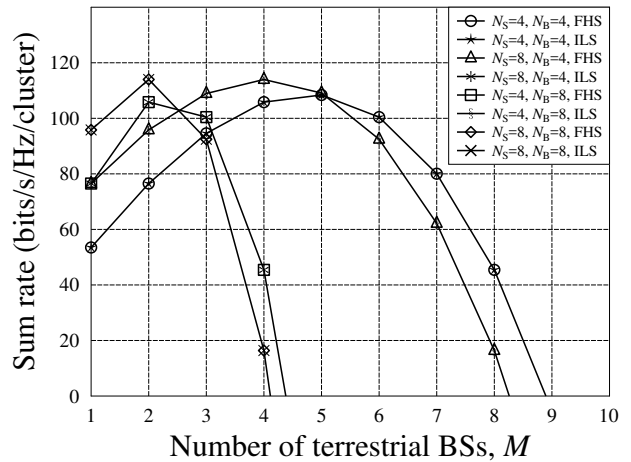


Fig. 5: The sum rate of a cluster in the CTSN under perfect CSI, where Gaussian codebooks are assumed to be employed. The number of satellite groups and terrestrial BS groups are $G_S = N_S$ and $G_B = MN_B$, respectively.

the performance loss imposed by the pilot overhead. Notably, as seen in Fig. 5, the sum rate performance of a given system setting is almost the same both in FHS and ILS scenarios. This is not unexpected since our proposed beamforming scheme is capable of providing a guaranteed SINR that is higher than γ_{\min} , as shown in (10). In other words, the satellite's antenna pattern can be carefully shaped by the proposed beamforming scheme so that the received SINRs experienced by all groups of ground users are similar in both the FHS and the ILS scenarios. Thus, as inferred from (30), almost the same sum rate can be attained by the satellite systems experiencing FHS and ILS.

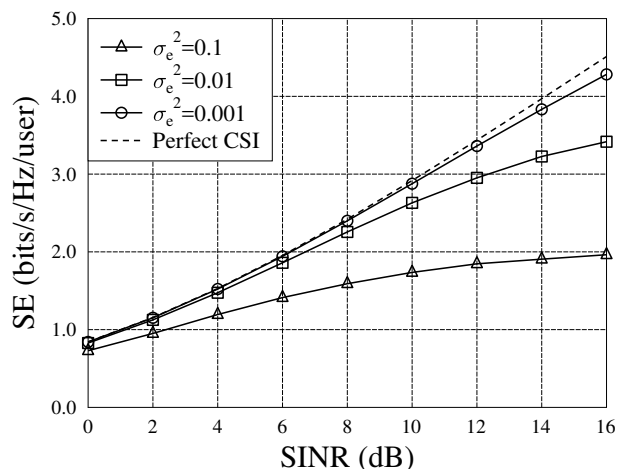


Fig. 6: SE versus the target SINR for CTSN systems under imperfect CSI, where Gaussian signalling waveforms are assumed. The satellite using $N_S = 8$ TAs supports $G_S = 4$ multicast groups. Two terrestrial BSs with $N_B = 8$ provide multicast services to $G_B = 8$ multicast groups. The variance of channel errors is $\sigma_e^2 = 0.001, 0.01, \text{ and } 0.1$.

In Fig. 6, we investigate the SE of the CTSN under imperfect CSI, where Gaussian signalling is assumed. In this figure, multicast services are provided by $G_S = 4$ satellite groups and $G_B = 8$ terrestrial BS groups. Each terrestrial BS is equipped with $N_B = 8$ TAs and $N_S = 8$ TAs of the satellite are employed for multicast transmission. The imperfect CSI model of Section III-B is used, where the variance of channel errors is $\sigma_e^2 = 0.001, 0.01, \text{ and } 0.1$. Observe from Fig. 6 that as expected the SE of the CTSN is reduced, when channel error variable is increased. This observation confirms our analysis of Section IV. As seen in (24) and (26), the received symbols at of both the satellite users and of the terrestrial BS users suffer from the inter-carrier interference imposed by the channel errors. Hence, the SINR experienced by the ground users becomes lower than the targeted value. As a result, the SE performance is reduced. Furthermore, it can be observed from (25), (27), and (29) that the higher the variance of channel errors, the lower the SE of the CTSN becomes.

VI. CONCLUSIONS

This paper studied multicast transmission aided CTSN, where the satellite and the terrestrial BSs are connected to the CP via their respective backhaul links. Specifically, beamforming has been invoked for implementing multicast transmission. In order to generate feasible beamforming vectors, a SCA-based algorithm has been conceived. We have shown that the proposed algorithm is capable of providing feasible solutions within a few iterations. Finally, both analytical and numerical results have been provided for evaluating the performance of the CTSN. The simulation results have shown that in order to provide a guaranteed SINR for all ground users, a higher transmission power is required by our system for combating the deleterious effects imposed by FHS in comparison to that imposed by ILS. We have shown that there is a tradeoff between the multiantenna gain and the pilot overhead. Hence, we have pointed out that the number of terrestrial BSs should be carefully chosen so that the achievable rate of the CTSN can be maximized. Furthermore, our results have shown that the attainable rate of the CTSN is dependent on the accuracy of CSI. Thus, high-performance CSI acquisition approaches are required by the CTSN for supporting high-speed multimedia transmission.

REFERENCES

- [1] T. de Cola, E. Paolini, G. Liva, and G. P. Calzolari, "Reliability options for data communications in the future deep-space missions," *Proceedings of the IEEE*, vol. 99, no. 11, pp. 2056–2074, Nov 2011.
- [2] C. Jiang, X. Wang, J. Wang, H. Chen, and Y. Ren, "Security in space information networks," *IEEE Communications Magazine*, vol. 53, no. 8, pp. 82–88, 2015.
- [3] J. Du, C. Jiang, Q. Guo, M. Guizani, and Y. Ren, "Cooperative earth observation through complex space information networks," *IEEE Wireless Communications*, vol. 23, no. 2, pp. 136–144, 2016.
- [4] J. Wang, C. Jiang, H. Zhang, V. Leung, and Y. Ren, "Aggressive congestion control mechanism for space systems," *IEEE Aerospace and Electronic Systems Magazine*, vol. 31, no. 3, pp. 28–33, 2016.
- [5] S. Maleki, S. Chatzinotas, B. Evans, K. Liolis, J. Grotz, A. Vanelli-Coralli, and N. Chuberre, "Cognitive spectrum utilization in Ka band multibeam satellite communications," *IEEE Communications Magazine*, vol. 53, no. 3, pp. 24–29, March 2015.
- [6] M. Sheng, Y. Wang, J. Li, R. Liu, D. Zhou, and L. He, "Toward a flexible and reconfigurable broadband satellite network: Resource management architecture and strategies," *IEEE Wireless Communications*, vol. 24, no. 4, pp. 127–133, 2017.
- [7] L. Kuang, C. Jiang, Y. Qiang, and J. Lu, *Terrestrial-Satellite Communication Networks*. Springer International Publishing, 2018.
- [8] D. Gesbert, S. Hanly, H. Huang, S. S. Shitz, O. Simeone, and W. Yu, "Multi-cell MIMO cooperative networks: A new look at interference," *IEEE Journal on Selected Areas in Communications*, vol. 28, no. 9, pp. 1380–1408, 2010.
- [9] A. Lozano, R. W. Heath, and J. G. Andrews, "Fundamental limits of cooperation," *IEEE Transactions on Information Theory*, vol. 59, no. 9, pp. 5213–5226, 2013.
- [10] J. Du, C. Jiang, Y. Qian, Z. Han, and Y. Ren, "Resource allocation with video traffic prediction in cloud-based space systems," *IEEE Transactions on Multimedia*, vol. 18, no. 5, pp. 820–830, 2016.
- [11] Y. Kawamoto, Z. M. Fadlullah, H. Nishiyama, N. Kato, and M. Toyoshima, "Prospects and challenges of context-aware multimedia content delivery in cooperative satellite and terrestrial networks," *IEEE Communications Magazine*, vol. 52, no. 6, pp. 55–61, June 2014.
- [12] C. Zhang, L. Kuang, and C. Jiang, "Spectrum sharing between geostationary and terrestrial communication systems," in *IEEE VTC' Spring*, June 2017, pp. 1–5.
- [13] X. Zhu, C. Jiang, W. Feng, L. Kuang, Z. Han, and J. Lu, "Resource allocation in spectrum-sharing cloud based integrated terrestrial-satellite network," in *International Wireless Communications and Mobile Computing Conference*, June 2017.
- [14] C. Jiang, X. Zhu, L. Kuang, Y. Qian, and J. Lu, "Multimedia multicast beamforming in integrated terrestrial-satellite networks," in *Proc. IEEE International Wireless Communications and Mobile Computing Conference (IWCMC)*, 2017, 2017.
- [15] C. Jiang, Y. Chen, Y. Gao, and K. J. R. Liu, "Joint spectrum sensing and access evolutionary game in cognitive radio networks," *IEEE Transactions on Wireless Communications*, vol. 12, no. 5, pp. 2470–2483, 2013.
- [16] C. Jiang, Y. Chen, K. J. R. Liu, and Y. Ren, "Renewal-theoretical dynamic spectrum access in cognitive radio network with unknown primary behavior," *IEEE Journal on Selected Areas in Communications*, vol. 31, no. 3, pp. 406–416, 2013.
- [17] H. Zhang, C. Jiang, L. Kuang, Y. Qian, and S. Guo, "Cooperative QoS beamforming for multicast transmission in terrestrial-satellite networks," in *2017 IEEE Global Communications Conference (GLOBECOM)*, Dec. 2017.
- [18] K. An, M. Lin, T. Liang, J. Wang, J. Wang, Y. Huang, and A. L. Swindlehurst, "Performance analysis of multi-antenna hybrid satellite-terrestrial relay networks in the presence of interference," *IEEE Transactions on Communications*, vol. 63, no. 11, pp. 4390–4404, Nov 2015.
- [19] T. S. Rappaport *et al.*, "Millimeter wave mobile communications for 5G cellular: It will work!" *IEEE Access*, vol. 1, no. 1, pp. 335–349, 2013.
- [20] X. Artiga, A. Perez-Neira, J. Baranda, E. Lagunas, S. Chatzinotas, R. Zetik, P. Gorski, K. Ntougias, D. Perez, and G. Ziaragkas, "Shared access satellite-terrestrial reconfigurable backhaul network enabled by smart antennas at MmWave band," *IEEE Network*, vol. 32, no. 5, pp. 46–53, Sep. 2018.
- [21] J. Du, C. Jiang, J. Wang, S. Yu, Z. Han, and Y. Ren, "Resource allocation in space multi-access systems," *IEEE Transactions on Aerospace and Electronic Systems*, vol. 53, no. 2, pp. 598–618, Apr. 2017.
- [22] Z. Lin, M. Lin, J. Wang, T. de Cola, and J. Wang, "Joint beamforming and power allocation for satellite-terrestrial integrated networks with non-orthogonal multiple access," *IEEE Journal of Selected Topics in Signal Processing*, vol. 13, no. 3, pp. 657–670, June 2019.
- [23] H. Liu, Z. Chen, X. Tian, X. Wang, and M. Tao, "On content-centric wireless delivery networks," *IEEE Wireless Communications*, vol. 21, no. 6, pp. 118–125, December 2014.
- [24] N. D. Sidiropoulos, T. N. Davidson, and Z.-Q. Luo, "Transmit beamforming for physical-layer multicasting," *IEEE Transactions on Signal Processing*, vol. 54, no. 6, pp. 2239–2251, June 2006.
- [25] E. Karipidis, N. D. Sidiropoulos, and Z. Q. Luo, "Quality of service and max-min fair transmit beamforming to multiple cochannel multicast groups," *IEEE Transactions on Signal Processing*, vol. 56, no. 3, pp. 1268–1279, March 2008.
- [26] Z. Xiang, M. Tao, and X. Wang, "Coordinated multicast beamforming in multicell networks," *IEEE Transactions on Wireless Communications*, vol. 12, no. 1, pp. 12–21, January 2013.
- [27] M. Tao, E. Chen, H. Zhou, and W. Yu, "Content-centric sparse multicast beamforming for cache-enabled cloud RAN," *IEEE Transactions on Wireless Communications*, vol. 15, no. 9, pp. 6118–6131, Sept 2016.

- [28] D. Christopoulos, S. Chatzinotas, and B. Ottersten, "Multicast multi-group precoding and user scheduling for frame-based satellite communications," *IEEE Transactions on Wireless Communications*, vol. 14, no. 9, pp. 4695–4707, Sept 2015.
- [29] M. A. Vazquez, A. Perez-Neira, D. Christopoulos, S. Chatzinotas, B. Ottersten, P. D. Arapoglou, A. Ginesi, and G. Tarocco, "Precoding in multibeam satellite communications: Present and future challenges," *IEEE Wireless Communications*, vol. 23, no. 6, pp. 88–95, 2015.
- [30] Z. Q. Luo, W. K. Ma, M. C. So, Y. Ye, and S. Zhang, "Semidefinite relaxation of quadratic optimization problems," *IEEE Signal Processing Magazine*, vol. 27, no. 3, pp. 20–34, 2010.
- [31] M. . Vazquez, A. Konar, L. Blanco, N. D. Sidiropoulos, and A. I. Prez-Neira, "Non-convex consensus admm for satellite precoder design," in *2017 IEEE International Conference on Acoustics, Speech and Signal Processing (ICASSP)*, March 2017, pp. 6279–6283.
- [32] B. R. Marks and G. P. Wright, "A general inner approximation algorithm for nonconvex mathematical programs," *Operations Research*, vol. 26, no. 4, pp. 681–683, 1978.
- [33] N. Bornhorst and M. Pesavento, "An iterative convex approximation approach for transmit beamforming in multi-group multicasting," in *Signal Processing Advances in Wireless Communications (SPAWC), 2011 IEEE 12th International Workshop on*. IEEE, 2011, pp. 426–430.
- [34] L. N. Tran, M. F. Hanif, and M. Juntti, "A conic quadratic programming approach to physical layer multicasting for large-scale antenna arrays," *IEEE Signal Processing Letters*, vol. 21, no. 1, pp. 114–117, Jan 2014.
- [35] O. Mehanna, K. Huang, B. Gopalakrishnan, A. Konar, and N. D. Sidiropoulos, "Feasible point pursuit and successive approximation of Non-Convex QCQPs," *IEEE Signal Processing Letters*, vol. 22, no. 7, pp. 804–808, July 2015.
- [36] D. Christopoulos, S. Chatzinotas, and B. Ottersten, "Multicast multi-group beamforming for per-antenna power constrained large-scale arrays," in *2015 IEEE 16th International Workshop on Signal Processing Advances in Wireless Communications (SPAWC)*, June 2015, pp. 271–275.
- [37] O. Tervo, L.-N. Tran, H. Pennanen, S. Chatzinotas, M. Juntti, and B. Ottersten, "Energy-efficient coordinated multi-cell multi-group multicast beamforming with antenna selection," in *2017 IEEE International Conference on Communications Workshops (ICC Workshops)*. IEEE, 2017, pp. 1209–1214.
- [38] A. Abdi, W. C. Lau, M. . Alouini, and M. Kaveh, "A new simple model for land mobile satellite channels: first- and second-order statistics," *IEEE Transactions on Wireless Communications*, vol. 2, no. 3, pp. 519–528, May 2003.
- [39] B. Hassibi and B. M. Hochwald, "How much training is needed in multiple-antenna wireless links?" *IEEE Transactions on Information Theory*, vol. 49, no. 4, pp. 951–963, 2003.
- [40] J. Zhang, B. Zhang, S. Chen, X. Mu, M. Elhajar, and L. Hanzo, "Pilot contamination elimination for large-scale multiple-antenna aided OFDM systems," *IEEE Journal of Selected Topics in Signal Processing*, vol. 8, no. 5, pp. 759–772, 2014.
- [41] E. Bjornson, E. G. Larsson, and T. L. Marzetta, "Massive MIMO: ten myths and one critical question," *IEEE Communications Magazine*, vol. 54, no. 2, pp. 114–123, 2015.